Ab Initio Characterization of $[H_3N{\cdot}BH_3]_2$, $[H_3N{\cdot}AlH_3]_2$, and $[H_3N{\cdot}GaH_3]_2$

Christopher J. Cramer* and Wayne L. Gladfelter*

Department of Chemistry and Supercomputer Institute, University of Minnesota, 207 Pleasant St. SE, Minneapolis, Minnesota 55455-0431

Received February 21, 1997[⊗]

The dimers of $[H_3N{\cdot}BH_3]_2$, $[H_3N{\cdot}AlH_3]_2$, and $[H_3N{\cdot}GaH_3]_2$ are characterized as head-to-tail complexes with intermolecular H−H hydrogen bonding. In the case of $[H_3N{\cdot}BH_3]_2$, that hydrogen bonding is bifurcated resulting in four short (N)H−H(B) distances. For both $[H_3N{\cdot}AlH_3]_2$ and $[H_3N{\cdot}GaH_3]_2$, there are only two short (N)H−H(Al/Ga) distances, although the four-atom linkage remains far from linear. The binding energies that are calculated at the MP2 level of theory using polarized-double-ζ basis sets are −15.1, −11.8, and −10.7 kcal/mol for $[H_3N{\cdot}BH_3]_2$, $[H_3N{\cdot}AlH_3]_2$, and $[H_3N{\cdot}GaH_3]_2$, respectively. These energies appear converged to within 1 kcal/mol with respect to larger basis sets and more complete accounting for electron correlation effects. Binding energies from density functional calculations are within 0.3 kcal/mol of the MP2 results. All-electron and effective-core-potential basis sets for gallium provide similar predictions.

Introduction

The hydrides of boron and aluminum are important to organic, inorganic, and materials chemistry. Somewhat less well studied, the hydrides of gallium are of growing importance.[1,2] For instance, in materials chemistry complexes such as dimethylethylamine−alane, $Me_2EtN{\cdot}AlH_3$, and trimethylamine−gallane, $Me_3N{\cdot}GaH_3$, have been used to prepare such solid state materials as aluminum,[3] aluminum gallium arsenide,[4] and gallium nitride.[5,6] In the last case, $Me_3N{\cdot}GaH_3$ was reacted with ammonia at low temperature to produce cyclotrigallazane, $[H_2GaNH_2]_3$, possibly via the unknown donor−acceptor complex $H_3N{\cdot}GaH_3$. Cyclotrigallazane was recently shown upon heating to produce nanocrystalline gallium nitride enriched in the zinc blende polymorph relative to the normal wurtzite structure.[6] The crystal structure of $[H_2GaNH_2]_3$ includes short NH−HGa contacts, indicating H−H hydrogen bonding to be taking place.[7] In order to quantify the energetic importance of this kind of interaction, we here undertake calculations on head-to-tail dimers of smaller group 13/group 15 complexes, namely, $[H_3N{\cdot}BH_3]_2$, $[H_3N{\cdot}AlH_3]_2$, and $[H_3N{\cdot}GaH_3]_2$.

These donor−acceptor complexes are also of interest for theoretical reasons.[8−15] For instance, $H_3N{\cdot}BH_3$ is isoelectronic with CH_3CH_3 (ethane), but the nature of the bonding between B and N is substantially different from that between C and C; the interaction is dative (or charge transfer) in the former instance and covalent in the latter. From the standpoint of theoretical technology, these complexes have also proven useful for quantifying the effects of using incomplete basis sets in calculations of the complex binding energy[16]—the qualitative observation is that using small basis sets can lead to a significant overestimation of the complexation energy, a phenomenon known as basis-set superposition error.[17−20] In addition to being of fundamental interest, the size of these systems allows high-level ab initio calculations to be carried out and these results used to benchmark more efficient levels of theory that may be useful in larger systems, e.g., dimers of cyclotrigallazane.

Theoretical Methods

All geometries were fully optimized at a variety of levels of theory, including Hartree−Fock (HF), Møller−Plesset perturbation theory complete through second order (MP2), and density functional theory (DFT). DFT calculations employed a combination of local, gradient-corrected, and exact exchange functionals according to the prescription of Becke[21,22] and the gradient-corrected correlation functional of Lee, Yang, and Parr (B3LYP).[23] Most calculations for $[H_3N{\cdot}BH_3]_2$ and $[H_3N{\cdot}AlH_3]_2$ and their corresponding monomers employed the correlation-consistent polarized valence-double-ζ (cc-pVDZ) basis set of Dunning and co-workers.[24,25] Select calculations also employed the correlation-consistent polarized core-and-valence-double-ζ[24−26] (cc-pCVDZ), augmented correlation-consistent polarized valence-double-ζ[24,25] (aug-cc-pVDZ), and correlation-consistent polarized valence-triple-ζ[24,25] (cc-pVTZ) basis sets of Dunning and co-workers. As the cc-pVDZ basis set was not extended to gallium at the time of these calculations, for $[H_3N{\cdot}GaH_3]_2$ and its monomer we employed the

⊗ Abstract published in *Advance ACS Abstracts,* October 15, 1997.

(1) Raston, C. L. *J. Organomet. Chem.* **1994**, *475*, 15.
(2) Downs, A. J.; Pulham, C. R. *Chem. Soc. Rev.* **1994**, *23*, 175.
(3) Simmonds, M. G.; Phillips, E. C.; Hwang, J.-W.; Gladfelter, W. L. *Chemtronics* **1991**, *5*, 155.
(4) Bohling, D. A.; Muhr, G. T.; Abernathy, C. R.; Jordan, A. S.; Pearton, S. J.; Hobson, W. S. *J. Cryst. Growth* **1991**, *107*, 1068.
(5) Hwang, J.-W.; Hanson, S. A.; Britton, D.; Evans, J. F.; Jensen, K. F.; Gladfelter, W. L. *Chem. Mater.* **1990**, *2*, 342.
(6) Hwang, J.-W.; Campbell, J. P.; Kozubowski, J.; Hanson, S. A.; Evans, J. F.; Gladfelter, W. L. *Chem. Mater.* **1995**, *7*, 517.
(7) Campbell, J. P.; Hwang, J.-W.; Young, V. G.; Von Dreele, R. B.; Cramer, C. J.; Gladfelter, W. L. To be published.
(8) Atwood, J. L.; Bennett, F. R.; Elms, F. M.; Jones, C.; Raston, C. L.; Robinson, K. D. *J. Am. Chem. Soc.* **1991**, *113*, 8183.
(9) Marsh, C. M. B.; Hamilton, T. P.; Xie, Y.; Schaefer, H. F., III. *J. Chem. Phys.* **1992**, *96*, 5310.
(10) Atwood, J. L.; Robinson, K. D.; Bennett, R. R.; Elms, F. M.; Koutsantonis, G. A.; Raston, C. L.; Young, D. J. *Inorg. Chem.* **1992**, *31*, 2674.
(11) Atwood, J. L.; Bennet, F. R.; Jones, C.; Koutsantonis, G. A.; Raston, C. L.; Robinson, K. D. *J. Chem. Soc., Chem. Commun.* **1992**, 541.
(12) Atwood, J. L.; Butz, K. W.; Gardiner, M. G.; Jones, C.; Koutsantonis, G. A.; Raston, C. L.; Robinson, K. D. *Inorg. Chem.* **1993**, *32*, 3482.
(13) Jungwirth, P.; Zahradník, R. *THEOCHEM* **1993**, *283*, 317.
(14) Holme, T. A.; Truong, T. N. *Chem. Phys. Lett.* **1993**, *215*, 53.
(15) Richardson, T. B.; de Gala, S.; Crabtree, R. H.; Siegbahn, P. E. M. *J. Am. Chem. Soc.* **1995**, *117*, 12875.
(16) Ahlrichs, R.; Koch, W. *Chem. Phys. Lett.* **1978**, *53*, 341.
(17) Boys, S. F.; Bernardi, F. *Mol. Phys.* **1970**, *19*, 553.
(18) Schwenke, D. W.; Truhlar, D. G. *J. Chem. Phys.* **1985**, *82*, 2418.
(19) Cammi, R.; Tomasi, J. *Theor. Chim. Acta* **1986**, *69*, 11.
(20) Davidson, E. R.; Chakravorty, S. J. *Chem. Phys. Lett.* **1994**, *217*, 48.
(21) Becke, A. D. *Phys. Rev. A* **1988**, *38*, 3098.
(22) Becke, A. D. *J. Chem. Phys.* **1993**, *98*, 5648.
(23) Lee, C.; Yang, W.; Parr, R. G. *Phys. Rev. B* **1988**, *37*, 785.
(24) Dunning, T. H. *J. Chem. Phys.* **1989**, *90*, 1007.
(25) Woon, D. E.; Dunning, T. H., Jr. *J. Chem. Phys.* **1993**, *98*, 1358.
(26) Woon, D.; Dunning, T. H., Jr. *J. Chem. Phys.* **1995**, *103*, 4572.

S0020-1669(97)00211-5 CCC: $14.00

Table 1. Geometrical Parameters for $H_3N{\cdot}BH_3$, $H_3N{\cdot}AlH_3$, and $H_3N{\cdot}GaH_3$[a–c]

molecule	level	*r*(XN)	*r*(XH)	*r*(NH)	∠NXH	∠XNH
$H_3N{\cdot}BH_3$, X = B	RHF	1.678	1.219	1.007	104.5	111.2
	B3LYP	1.654	1.222	1.023	104.9	111.6
	MP2	1.656	1.223	1.023	104.8	111.5
	expt[d]	1.672	1.210	1.014	104.5	109.9
$H_3N{\cdot}AlH_3$, X = Al	RHF	2.121	1.605	1.009	99.3	111.7
	B3LYP	2.111	1.606	1.024	99.0	112.0
	MP2	2.116	1.602	1.024	99.0	112.3
$H_3N{\cdot}GaH_3$, X = Ga	RHF[e]	2.200	1.591	1.008	98.4	111.7
	B3LYP[e]	2.184	1.585	1.023	98.0	111.8
	MP2[e]	2.163	1.574	1.024	98.4	112.2
	RHF[f]	2.192	1.579	1.009	98.5	111.8
	B3LYP[f]	2.185	1.586	1.024	98.3	112.2
	MP2[f]	2.182	1.574	1.024	98.0	112.6

[a] Bond lengths in Å; bond angles in deg. [b] All structures have C_{3V} symmetry. [c] Calculations used the cc-pVDZ basis set unless otherwise indicated. [d] Reference 32. [e] pVDZ basis set. [f] pVDZ basis set for H and N; ECP for Ga.

Table 2. Selected Geometrical Parameters for $[H_3N{\cdot}BH_3]_2$, $[H_3N{\cdot}AlH_3]_2$, and $[H_3N{\cdot}GaH_3]_2$[a–c]

molecule	level	*r*(XN)	*r*(XH)	*r*(NH)	*r*(HH)	∠XHH	∠NHH
$[H_3N{\cdot}BH_3]_2$, X = B	RHF	1.650	1.225	1.007	2.194	91.7	147.0
	B3LYP	1.629	1.228	1.034	1.985	87.9	145.5
	MP2	1.632	1.228	1.031	1.990	88.6	144.8
$[H_3N{\cdot}AlH_3]_2$, X = Al	RHF	2.091	1.600	1.013	2.000	133.4	165.0
	B3LYP	2.075	1.627	1.024	1.706	132.3	172.6
	MP2	2.081	1.620	1.035	1.781	119.4	172.0
$[H_3N{\cdot}GaH_3]_2$, X = Ga	RHF[d]	2.162	1.605	1.012	2.088	130.0	163.3
	B3LYP[d]	2.140	1.581	1.034	1.784	123.9	171.7
	MP2[d]	2.122	1.567	1.031	1.898	108.3	178.0
	RHF[e]	2.156	1.594	1.012	2.067	134.4	164.9
	B3LYP[e]	2.141	1.608	1.036	1.760	133.2	172.8
	MP2[e]	2.141	1.594	1.032	1.804	131.8	173.2

[a] Bond lengths in Å; bond angles in deg; hydrogen atoms referred to are those involved in H−H hydrogen bonding. [b] $[H_3N{\cdot}BH_3]_2$ has C_{2h} symmetry, and $[H_3N{\cdot}AlH_3]_2$ and $[H_3N{\cdot}GaH_3]_2$ have C_2 symmetry. [c] Calculations used the cc-pVDZ basis set unless otherwise indicated. [d] pVDZ basis set. [e] pVDZ basis set for H and N; ECP for Ga.

polarized valence-double-ζ (pVDZ) basis set[27] of Schafer et al. for all atoms. In addition, since our longer range goals include exploring considerably larger analogs of these systems, more efficient calculations for $[H_3N{\cdot}GaH_3]_2$ and its monomer were carried out replacing the all-electron pVDZ basis set for gallium with the effective-core-potential valence-double-ζ basis set[28] (ECP) of Hay and Wadt. For $[H_3N{\cdot}BH_3]_2$, $[H_3N{\cdot}AlH_3]_2$, and their respective monomers, single-point calculations were carried out accounting for electron correlation with coupled-cluster theory including all single and double excitations with triple excitations estimated perturbatively (CCSD(T)).[29,30]

All stationary points were characterized by calculation of analytic force constants with the exception of structures calculated with the ECP basis set. For each geometry (HF, DFT, or MP2), single-point calculations were carried out with the other two methods. All calculations used the Gaussian 94 suite of electronic structure programs.[31]

Results

$[H_3N{\cdot}BH_3]_2$. Table 1 contains structural data for monomeric $H_3N{\cdot}BH_3$ (C_{3v}), and Table 2 contains structural data for $[H_3N{\cdot}BH_3]_2$ (C_{2h}), which is a head-to-tail dimer of $H_3N{\cdot}BH_3$ that exhibits two sets of bifurcated H−H hydrogen bonds involving one N−H hydrogen and two B−H hydrogens. Figure 1 illustrates stereostructures for these compounds as calculated at the MP2 level. For the monomer, all three levels of theory give reasonable agreement with experiment.[32] The apparent utility of DFT in describing donor−acceptor complexes such as $H_3N{\cdot}BH_3$ has previously been noted by Holme and Truong (who also provide a comprehensive listing of other theoretical studies of $H_3N{\cdot}BH_3$).[14]

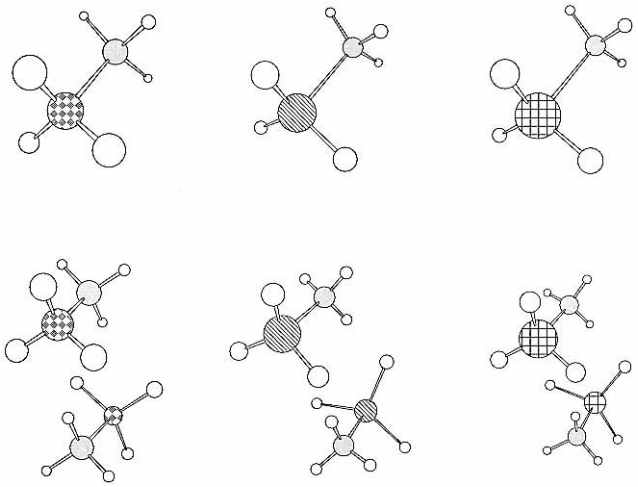

Figure 1. From left to right, stereostructures of monomeric (above) and dimeric (below) $H_3N{\cdot}BH_3$, $H_3N{\cdot}AlH_3$, and $H_3N{\cdot}GaH_3$ from MP2 calculations (cc-pVDZ basis set for $H_3N{\cdot}XH_3$, X = B and X = Al; pVDZ basis set for X = Ga).

Crabtree et al.[15] have previously communicated calculations on $[H_3N{\cdot}BH_3]_2$. Although details were somewhat sketchy, they

(27) Schafer, A.; Horn, H.; Ahlrichs, R. *J. Chem. Phys.* **1992**, *97*, 2571.
(28) Hay, P. J.; Wadt, W. R. *J. Chem. Phys.* **1985**, *82*, 270.
(29) Cizek, J. *Adv. Chem. Phys.* **1969**, *14*, 35.
(30) Purvis, G. D.; Bartlett, R. J. *J. Chem. Phys.* **1982**, *76*, 1910.
(31) Frisch, M. J.; Trucks, G. W.; Schlegel, H. B.; Gill, P. M. W.; Johnson, B. G.; Robb, M. A.; Cheeseman, J. R.; Keith, T.; Petersson, G. A.; Montgomery, J. A.; Raghavachari, K.; Al-Laham, M. A.; Zakrzewski, V. G.; Ortiz, J. V.; Foresman, J. B.; Cioslowski, J.; Stefanov, B. B.; Nanayakkara, A.; Challacombe, M.; Peng, C. Y.; Ayala, P. Y.; Chen, W.; Wong, M. W.; Andres, J. L.; Replogle, E. S.; Gomperts, R.; Martin, R. L.; Fox, D. J.; Binkley, J. S.; Defrees, D. J.; Baker, J.; Stewart, J. P.; Head-Gordon, M.; Gonzalez, C.; Pople, J. A. *Gaussian 94*, Rev D.1; Gaussian Inc.: Pittsburgh, PA, 1995.
(32) Thorne, L. R.; Suenrum, R. D.; Lovas, F. J. *J. Chem. Phys.* **1983**, *78*, 167.

Table 3. Dimerization Energies (kcal/mol) for $[H_3N{\cdot}BH_3]_2$, $[H_3N{\cdot}AlH_3]_2$, and $[H_3N{\cdot}GaH_3]_2$[a]

		geometry		
molecule	energy	RHF	B3LYP	MP2
$[H_3N{\cdot}BH_3]_2$	RHF	−10.3	−9.2	−9.3
	B3LYP	−13.4	−14.4	−14.4
	MP2	−14.3	−15.1	−15.1
$[H_3N{\cdot}AlH_3]_2$	RHF	−8.3	−6.9	−7.2
	B3LYP	−10.6	−11.8	−11.6
	MP2	−10.9	−11.6	−11.8
$[H_3N{\cdot}GaH_3]_2$	RHF[b]	−6.9	−5.5	−5.6
	B3LYP[b]	−8.7	−9.9	−9.5
	MP2[b]	−9.6	−10.4	−10.7
	RHF[c]	−7.1	−5.7	−6.2
	B3LYP[c]	−9.0	−10.1	−10.0
	MP2[c]	−9.5	−10.2	−10.2

[a] Calculations used the cc-pVDZ basis set unless otherwise indicated. [b] pVDZ basis set used for energies and geometries. [c] pVDZ basis set for H and N and ECP for Ga used for energies and geometries.

reported a C_2 structure from both DFT (B3LYP, the same functional used in this study) and MP2 optimizations using double-ζ basis sets. The C_2 structure they reported is overall rather similar to the geometries we find for $[H_3N{\cdot}AlH_3]_2$ and $[H_3N{\cdot}GaH_3]_2$ (vide infra; see also Figure 1). However, all of our attempts to converge to such a structure at HF, DFT, or MP2 levels of theory led smoothly to the C_{2h} structures reported in Table 1.

The potential surface associated with the motion that would interconvert two enantiomeric C_2 structures through a C_{2h} intermediate is remarkably flat, however, and this may lead to the apparent discrepancy between our current results and those obtained by Crabtree et al.[15] In particular, we calculated the C_2 structure reported by Crabtree et al.[15,33] to be only 0.2 kcal/mol higher in energy than our optimized C_{2h} structure at the B3LYP/cc-pVDZ level. Subsequent optimization led to the structure relaxing to C_{2h}. The separate findings of two quite different optimized geometries may be due to the use of different algorithms for geometry optimization or possibly to slight differences in the double-ζ basis sets (albeit we found use of the cc-pCVDZ and aug-cc-pVDZ basis sets to continue to predict a C_{2h} geometry), but it is clear that, given the flat nature of the potential energy surface, this observation is without chemical consequence. Vibrational motion would be expected to sample a broad range of the torsional coordinate associated with this geometric descriptor (the harmonic frequency associated with this normal mode is 89 cm^{-1}); infrared frequencies calculated for $[H_3N{\cdot}BH_3]_2$ at the B3LYP/cc-pVDZ level are provided in the Supporting Information.

The absolute energies for $H_3N{\cdot}BH_3$ and $[H_3N{\cdot}BH_3]_2$ are provided in the Supporting Information, and the binding energies of the dimer for various levels of theory and different geometries are provided in Table 3. Because of the bifurcated nature of the hydrogen bonding in $[H_3N{\cdot}BH_3]_2$, we also examined the alternative head-to-tail bifurcated structure, i.e., having each of two hydrogen atoms attached to boron making two contacts with hydrogen atoms attached to nitrogen. Since the electron density associated with the B−H bonds is located primarily between the two atoms (as opposed to looking like a "lone pair" on hydrogen), one would not a priori expect this to be an especially favorable geometry for H−H hydrogen bonding, and indeed it is not. The alternative C_{2h} dimer is a hilltop on the potential energy surface (two imaginary frequencies).

$[H_3N{\cdot}AlH_3]_2$. Table 1 contains structural data for monomeric $H_3N{\cdot}AlH_3$ (C_{3v}), and Table 2 contains structural data for $[H_3N{\cdot}AlH_3]_2$ (C_2), which is a head-to-tail dimer of $H_3N{\cdot}AlH_3$ that twists the two Al−N bonds relative to one another in order to form two H−H hydrogen bonds involving one N−H hydrogen and one Al−H hydrogen. Figure 1 illustrates stereostructures for these compounds as calculated at the MP2 level. The monomer geometry is consistent with previous calculations;[8,9,11,12] an experimental geometry for the monomer is not available.

For the dimer, attempts to locate an alternative C_2 structure where the AlH−HN bonding pattern would be reversed were unsuccessful, all geometries smoothly converging to the one shown in Figure 1. In addition, when the molecular geometry was constrained to be C_{2h}, analogous to the $[H_3N{\cdot}BH_3]_2$ structure, a force constant calculation revealed two imaginary frequencies corresponding to coupled rotations about the two Al−N bonds to return the structure to C_2 symmetry. Atwood et al.[8] have shown experimentally and computationally that hydride-bridged dimers of hypervalent aluminum are available to $R_3N{\cdot}AlH_3$ compounds. However, we have not considered that dimerization motif here since it is not relevant for the other two systems (vide infra). Infrared frequencies for the minimum-energy structure are given in the Supporting Information, as are absolute energies for monomeric $H_3N{\cdot}AlH_3$ and for $[H_3N{\cdot}AlH_3]_2$. The dimerization energies at various levels are given in Table 3.

$[H_3N{\cdot}GaH_3]_2$. Table 1 contains structural data for monomeric $H_3N{\cdot}GaH_3$ (C_{3v}), and Table 2 contains structural data for $[H_3N{\cdot}GaH_3]_2$ (C_2), which is a head-to-tail dimer of $H_3N{\cdot}GaH_3$ closely resembling the structure found for $[H_3N{\cdot}AlH_3]_2$. Figure 1 illustrates stereostructures for the gallium species. The various calculations were all performed using both the all-electron pVDZ basis and substituting the double-ζ ECP basis for gallium, and both sets of results may be found in the relevant tables. Atwood et al.[10] previously reported all-electron MP2 calculations on $H_3N{\cdot}GaH_3$ predicting Ga−N and Ga−H bond lengths of 2.074 and 1.570 Å, respectively. Our absolute energy is about 0.7 hartree lower than their reported value, suggesting our basis set to be more complete and thus our 0.09 Å longer Ga−N bond length to be more accurate. All other aspects of this system were quite similar to the aluminum case, e.g., no evidence for an alternative C_2 structure, two imaginary frequencies calculated for the C_{2h} structure, etc. Atwood et al.[10] searched for a hydride-bridged dimer of $H_3N{\cdot}GaH_3$ analogous to that found for the alane case[8] and concluded that one did not exist. Infrared frequencies for the minimum-energy structure are given in the Supporting Information, as are absolute energies for monomeric $H_3N{\cdot}GaH_3$ and for $[H_3N{\cdot}GaH_3]_2$. The dimerization energies at various levels are given in Table 3.

Discussion

Theoretical Models. We begin by examining the performances of the different levels of theory because it will render the discussion of structural and energetic consequences of dimerization more efficient if we focus only on the "best" level of theory and also because one of our goals is to identify the suitability of less expensive methods for studying larger analogs of the $XH_3{\cdot}NH_3$ dimers. There are several general trends that emerge from the calculations. In both monomers and dimers, RHF calculations consistently overestimate B−N bond lengths by about 0.02 Å and N−H bond lengths by a similar amount compared to B3LYP or MP2. Although not observed in the monomers, there are discrepancies of 0.02−0.03 Å in the RHF hydrogen-bonded X−H bond lengths compared to B3LYP and MP2 for the aluminum and gallium dimers (the latter only for the all-electron basis set). The largest difference, however, is in the calculation of the H−H distances in the dimers, where

(33) Siegbahn, P. E. M. Personal communication.

RHF structures are consistently about 0.2 Å further apart than MP2 structures. The agreement between B3LYP and MP2 is closer, although in the case of $[H_3N{\cdot}GaH_3]_2$ with the all-electron pVDZ basis, the DFT structure has H−H distances 0.1 Å shorter than those in the MP2 structure.

The bond angles across the XH−HN linkage are also very sensitive to the theoretical level. While all levels agree reasonably well on the $[H_3N{\cdot}BH_3]_2$ structure, the RHF level always predicts a more acute NHH angle for the remaining dimers by 7−15°, and the MP2 level predicts up to 22° more acute XHH bond angles than either B3LYP or RHF for the remaining dimers when all-electron basis sets are used. Interestingly, structural agreement between the three levels for $[H_3N{\cdot}GaH_3]_2$ is improved for the ECP basis set compared to the all-electron basis. In general, comparing the all-electron gallium structures to the ECP structures, there is quite good agreement between the two at the RHF and B3LYP levels of theory for all parameters except the Ga−H bond length in the dimers, which changes by up to 0.027 Å. The MP2 dimer shows somewhat more sensitivity to basis set, with the H−H bond distance changing by 0.094 Å and the XHH bond angle changing by 23.5° (these changes presumably being strongly coupled).

However, while there is variability in the structures as a function of theoretical level, there is very little difference in the B3LYP and MP2 absolute energies calculated for either one of those two geometries; i.e., the geometric differences are associated with degrees of freedom having relatively flat potentials. Thus, for all molecules except $[H_3N{\cdot}GaH_3]_2$, the difference between either the B3LYP or MP2 energies calculated for either geometry is less than 0.2 kcal/mol. For $[H_3N{\cdot}GaH_3]_2$ with the all-electron pVDZ basis, there is a 0.6 kcal/mol difference in the B3LYP energies depending on which geometry is used, while for MP2 the difference is 0.4 kcal/mol. As noted above, with the ECP basis the B3LYP and MP2 geometries are in better agreement and the energetic differences are reduced to 0.2 kcal/mol, about the same amount observed for the other dimers.

The RHF level of theory, on the other hand, predicts substantially larger interdimer distances, as already noted above. The repulsive potential at the RHF level of theory associated with reducing this separation is fairly steep; in general, absolute RHF energies for the B3LYP and MP2 structures are 2−3 kcal/mol higher in energy than those for the RHF structures. From the opposite standpoint, the *attractive* potentials at the B3LYP and MP2 levels of theory are *not* as steep. Thus, B3LYP and MP2 binding energies are reduced by only about 1 kcal/mol when the RHF structures are used as opposed to those from the correlated levels. This suggests that RHF structures, which are considerably less expensive to determine than B3LYP or MP2 structures, may be useful for single-point calculations of larger analogs[7] provided small corrections are made for the slightly reduced interaction energies at longer distances.

The absolute dimerization energies are predicted to be very similar by the B3LYP and MP2 levels for a given geometry—typically the agreement is within 1 kcal/mol. The RHF level, on the other hand, predicts dimerization energies that are about 2 kcal/mol smaller than those found at the correlated levels for RHF geometries and 3−5 kcal/mol smaller for the B3LYP or MP2 geometries. A portion of this effect can be ascribed to the inability of the RHF level of theory to account for attractive dispersion forces between the two monomers.

Because of the weak nature of the intermolecular interaction, we examined the effect of adding diffuse functions to the basis set (heavy and light atoms) for both $[H_3N{\cdot}BH_3]_2$ and $[H_3N{\cdot}AlH_3]_2$. In the latter instance, the effects of diffuse functions were negligible—in particular, at the B3LYP/aug-cc-pVDZ level of theory the dimerization energy is unchanged and the intermolecular H−H hydrogen bond lengthens by 0.001 Å (the largest change in any bond length in the dimer is 0.004 Å and bond angles are similarly affected only marginally). For $[H_3N{\cdot}BH_3]_2$, on the other hand, the bifurcated hydrogen bonds are slightly more sensitive to this improvement in the basis set, and the intermolecular H−H hydrogen bond lengthens by 0.018 Å while the dimerization energy drops by 0.9 kcal/mol. This is an interesting consequence of the difference in the hydrogen-bonding motif for the two dimers, but the effects are sufficiently small for $[H_3N{\cdot}BH_3]_2$ that for the sake of consistency we will continue to consider primarily results from using the cc-pVDZ basis set.

To further evaluate the sensitivity of the dimerization energies to basis set, we also carried out B3LYP and MP2 optimizations for $H_3N{\cdot}BH_3$ and $[H_3N{\cdot}BH_3]_2$ using the cc-pVTZ basis set (264 basis functions compared to 116 basis functions for cc-pVDZ). The B3LYP dimerization energy reduces to −12.7 kcal/mol, while the MP2 dimerization energy increases slightly to −15.4. DFT methods have not been extensively tested for the calculation of intermolecular interaction energies,[34] and in a few instances they have been shown to give erroneous results from an apparent bias toward favoring charge transfer,[35] so we consider the MP2 method to probably be the most reliable and the convergence of the dimerization energy with respect to basis set to be legitimate. We also tested the sensitivity of the dimerization energy to further accounting for electron correlation by carrying out CCSD(T)/cc-pVDZ calculations for $[H_3N{\cdot}BH_3]_2$ and $[H_3N{\cdot}AlH_3]_2$ and their respective monomers at MP2 geometries. The dimerization energy is reduced by 0.4 kcal/mol for $[H_3N{\cdot}BH_3]_2$ and by 0.2 kcal/mol for $[H_3N{\cdot}AlH_3]_2$, suggesting that the MP2 level adequately accounts for electron correlation effects in these systems. As a result, we will confine the remainder of the discussion to MP2 results, and we note that, for future studies of larger analogs, we expect MP2/pVDZ calculations at RHF/pVDZ geometries will provide dimerization energies only about 0.5 kcal/mol per H−H hydrogen bond lower than what would be predicted from full MP2/pVDZ optimizations, which would themselves be expected to show reasonable quantitative accuracy.

Although we did not examine the sensitivity of $[H_3N{\cdot}GaH_3]_2$ to the same expanded basis set and correlation effects described above, because of its structural similarity to $[H_3N{\cdot}AlH_3]_2$ we consider it unlikely that $[H_3N{\cdot}GaH_3]_2$ would behave any differently. We also note that the dimerization energies calculated for $[H_3N{\cdot}GaH_3]_2$ are all within 0.5 kcal/mol of those calculated with the all-electron pVDZ basis, suggesting that use of an ECP basis for gallium can be used to increase the efficiency of calculations on larger analogs with little loss of accuracy.

Molecular Geometries. The monomer geometries are unremarkable and exhibit the expected bond lengths and angles for these donor−acceptor complexes.[8−15] Upon dimerization, the X−N dative bonds all shorten, with the effect being largest for $H_3N{\cdot}GaH_3$ (0.041 Å with either the pVDZ or ECP basis set) and smallest for $H_3N{\cdot}BH_3$ (0.024 Å). This probably reflects greater charge transfer from nitrogen to the group 13 atom that is stabilized either directly by the H−H hydrogen-bonding interaction or more generally by the creation of opposing X−N bond dipoles in the dimer structures. The N−H bonds involved in the H−H hydrogen-bonding interaction are longer in the

(34) Sim, F.; St-Amant, F. A.; Papai, I.; Salahub, D. R. *J. Am. Chem. Soc.* **1992**, *114*, 4391.
(35) Ruiz, E.; Salahub, D.; Vela, A. *J. Am. Chem. Soc.* **1995**, *117*, 1141.

dimers than in the monomers by about 0.01 Å; no such lengthening is observed for the noninteracting N−H bonds. The trend in X−H bonds is more variable, with $H_3N{\cdot}GaH_3$ showing some sensitivity to the pVDZ vs ECP basis set.

As for trends among the dimers themselves, the H−H hydrogen bond lengths are shortest for $[H_3N{\cdot}AlH_3]_2$ (1.781 Å), longer for $[H_3N{\cdot}GaH_3]_2$ (with again some sensitivity to pVDZ vs ECP basis set), and longest for $[H_3N{\cdot}BH_3]_2$ (1.990 Å), where the hydrogen-bonding interactions are bifurcated. It may be that the bifurcated hydrogen bonding is present in the last case because the short nature of the B−H bonds, compared to Al−H or Ga−H, allows the maximum negative charge density for two B−H bonds to be sufficiently close for one proton to interact efficiently with both.

It is not clear that it is profitable to analyze the trends in XHH and NHH bond angles across the H−H hydrogen bond since the potential energy curves associated with these coordinates appear to be so flat. As Crabtree et al.[15] pointed out on the basis of an analysis of crystallographic data and calculations on $[H_3N{\cdot}BH_3]_2$, the XHH angle is acute while the NHH angle more nearly approaches linearity because the position of maximum electronic charge in the X−H bonds is *between* the two atoms, while the maximum *depletion* of charge in the vicinity of a hydrogen atom bound to nitrogen is located *outside* the bonding region of the N−H bond.

Dimerization Energies. The largest predicted dimerization energy is for $[H_3N{\cdot}BH_3]_2$ at −15.1 kcal/mol, the next largest is for $[H_3N{\cdot}AlH_3]_2$ at −11.8 kcal/mol, and the smallest is for $[H_3N{\cdot}GaH_3]_2$ at −10.7 kcal/mol (−10.2 kcal/mol with the ECP basis set). The large drop from boron to aluminum and the subsequently smaller drop for gallium probably reflect the degree to which negative charge density is concentrated in space about the group 13 hydride fragments. With short B−H bonds, there is maximal concentration of charge for $[H_3N{\cdot}BH_3]_2$. The Al−H bonds in $[H_3N{\cdot}AlH_3]_2$ are somewhat longer than the Ga−H bonds in $[H_3N{\cdot}GaH_3]_2$, but since the dimerization energies of the last two complexes differ only marginally, it is probably not worthwhile to attempt to rationalize this. In any case, for the heavier group 13 elements, it is apparent that each H−H hydrogen bond involving an N−H proton has an energy on the order of 5−6 kcal/mol, squarely in the range of hydrogen-bonding energies expected for more typical N−H interactions with oxygen and nitrogen lone pairs.

Conclusions

$H_3N{\cdot}BH_3$, $H_3N{\cdot}AlH_3$, and $H_3N{\cdot}GaH_3$ form head-to-tail dimers exhibiting intermolecular H−H hydrogen bonding. That hydrogen bonding is bifurcated for C_{2h} $[H_3N{\cdot}BH_3]_2$ and nonlinear (but not bifurcated) for C_2 $[H_3N{\cdot}AlH_3]_2$ and $[H_3N{\cdot}GaH_3]_2$. Dimerization energies appear reasonably well converged with respect to basis set and correlation at the MP2 level of theory using polarized-double-ζ basis sets; those dimerization energies are −15.1, −11.8, and −10.7 kcal/mol for $[H_3N{\cdot}BH_3]_2$, $[H_3N{\cdot}AlH_3]_2$, and $[H_3N{\cdot}GaH_3]_2$, respectively. Density functional calculations give very similar results but seem somewhat more sensitive to basis set. RHF calculations give dimer geometries that are considerably looser than those found at correlated levels of theory, but correlated dimerization energies for these structures are typically only reduced relative to fully optimized structures by about 0.5 kcal/mol per hydrogen bond, suggesting that such calculations might be a useful alternative in systems too large to efficiently optimize at correlated levels. For gallium, structural and energetic results from calculations employing effective core potentials are consistent with those derived from all-electron basis sets, suggesting that effective core potentials may also be an efficient choice in larger systems.

Acknowledgment. We are grateful for high-performance vector and parallel computing resources made available by the Minnesota Supercomputer Institute and the University of Minnesota-IBM Shared Research Project, respectively. C.J.C. thanks the Alfred P. Sloan foundation for funding. Professor P. E. M. Siegbahn graciously provided us with coordinates for the dimer of $H_3N{\cdot}BH_3$ reported in ref 15.

Supporting Information Available: Listings of calculated infrared frequencies for all dimers and absolute energies (E_h) for all monomers and dimers (3 pages). Ordering information is given on any current masthead page.

IC970211D